Validity of the discrete nonlinear Schrödinger equation in the context of the fluorescence depolarization of a spin-boson system

S. Raghavan and V. M. Kenkre

Center for Advanced Studies, Department of Physics and Astronomy, University of New Mexico, Albuquerque, New Mexico 87131

A. R. Bishop and M. I. Salkola[*]

Theoretical Division and Center for Nonlinear Studies, Los Alamos National Laboratory, Los Alamos, New Mexico 87545

The validity of the discrete nonlinear Schrödinger equation and related semi-classical transport equations is studied with the help of an exact calculation of the spin-boson system in the experimentally relevant context of the fluorescence depolarization of stick dimers. The consequences of an initial excitation corresponding to low-energy dynamics are investigated. A number of features are found including the sensitive role of the polarization angle of incident light in determining the regimes of validity. Our earlier finding that the semi-classical approximation improves in validity in a well defined "massive oscillator" limit involving small phonon frequency is borne out. In the opposite limit of large phonon frequency, the semiclassical approximation and the discrete nonlinear Schrödinger equation are found to coincide with each other but to differ significantly from the exact evolution.

Strong interactions of quasiparticles such as electronic excitations with vibrations pose a fundamental problem which is of interest in many systems.[1-3] Semiclassical approximations including the discrete nonlinear Schrödinger equation (DNLSE) have been often used for the description of these systems.[4-9] Questions concerning the validity of the semiclassical approximation have been raised[10-13] and serious doubts have been cast on the effects that the semiclassical approximation and the DNLSE have predicted.[10-12] We have recently reported on the validity of the semiclassical approximation as applied specifically to a dimer interacting with one mode of vibration[14,15] and identified a well-defined limit in which the semiclassical approximation is an exact outcome of the fully quantum evolution. In the present paper, we investigate the validity of the consequences of the DNLSE and what is termed *the* semiclassical approximation (SCA) (Ref. 16) in the context of a specific experimental observable, viz., fluorescence depolarization.

That fluorescence depolarization provides an excellent experimental tool for probing the nonlinear transport of excitations in interaction with vibrations has been shown clearly in a recent report[17] in which the basic observable, viz., the degree of fluorescence depolarization f has been calculated for a variety of (nonlinear) transport equations ranging from the simple linear limit to one involving thermal fluctuations and dissipation. For details we refer the reader to Ref. 17. The fundamental ideas and expressions are as follows. The system is a collection of "stick dimers" which consist of poly-L-proline oligomers of controllable length that are used to separate an α-naphthyl group at the carboxyl end (the donor) from the dansyl group at the imino end (the acceptor).[16-21] Polarized light is used to create electronic excitations in the system and the depolarization of emitted light is studied. See Fig. 1. The basic time-resolved observable $f(t)$ is given by

$$f(t)=[I_{\parallel}(t)-I_{\perp}(t)]/[I_{\parallel}(t)+I_{\perp}(t)]=p\,\cos2\phi+r\,\sin2\phi, \tag{1}$$

where $I_{\parallel}(t)$ and $I_{\perp}(t)$ are the differential photon count rates parallel and perpendicular to the direction of the incident light polarization, ϕ is the angle made by the polarization of the incident light with the induced dipole moment on molecule 1, the induced dipole moments on the two molecules are assumed to be mutually perpendicular for simplicity, and p and r are two of the three density matrix elements of the excitation in the basis of the sites (1,2) of the dimer:

$$p=\rho_{11}-\rho_{22}; \quad q=i(\rho_{12}-\rho_{21}); \quad r=\rho_{12}+\rho_{21}. \tag{2}$$

The dimer is represented by the Hamiltonian

$$\hat{H}=V\hat{r}+\hbar g\,\omega\hat{y}\hat{p}+\frac{1}{2}\,\hbar\,\omega(\hat{y}^2+\hat{\pi}_y^2), \tag{3}$$

where the quasiparticle electronic excitation operators $\hat{p},\hat{q},\hat{r}$ are defined as $\hat{p}=a_1^{\dagger}a_1-a_2^{\dagger}a_2$, $\hat{q}=-i(a_1^{\dagger}a_2-a_2^{\dagger}a_1)$, and $\hat{r}=a_1^{\dagger}a_2+a_2^{\dagger}a_1$. The operators $\hat{y}$ and $\hat{\pi}_y$ obey the commuta-
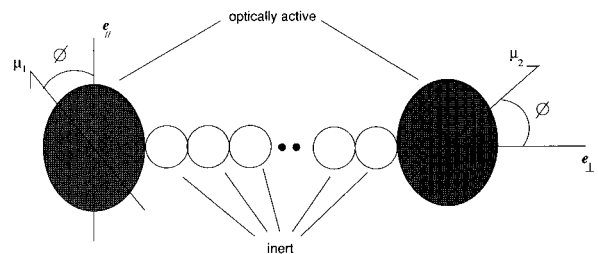

FIG. 1. Schematic of the fluorescence depolarization of a molecular dimer. The circles at the two ends, shown shaded, indicate optically active molecules which give rise to electronic excitation upon the incidence of light. The circles that are unshaded, indicate optically inert molecules. The angled arrows denote the two induced dipole moments on each optically active molecule: μ_1, μ_2 are the dipole moments. The polarization vector $e_{\parallel}$ is shown to be at an angle ϕ with one of the dipole moments, μ_1. The dark circles in the middle show the variable number of inert molecules.
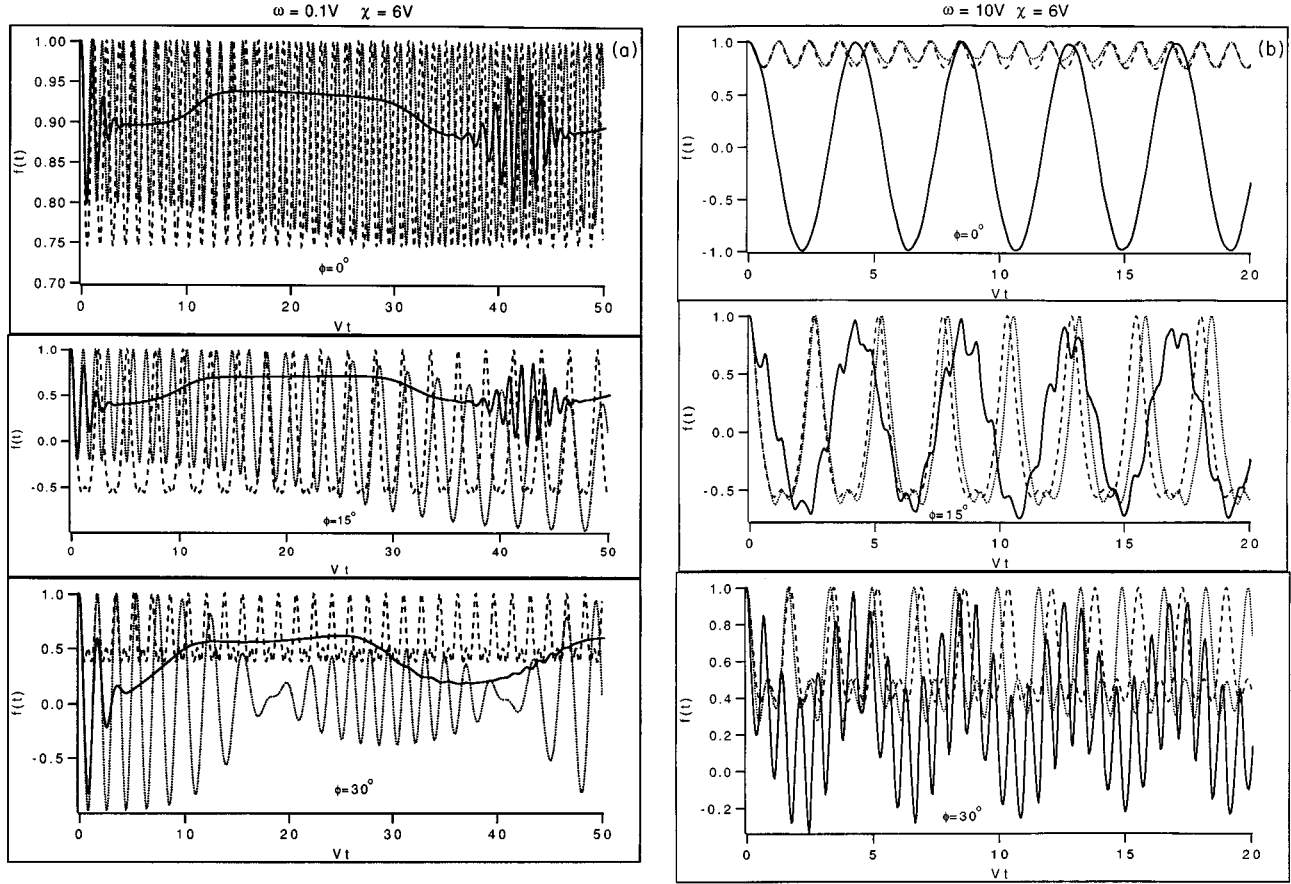
FIG. 2. Comparison of the predictions for time-resolved fluorescence polarization from (i) the exact numerical analysis (solid line), (ii) the semiclassical treatment (dotted line), and (iii) the DNLSE approximation (dashed line) for three values of the inclination, $\phi=0°,15°,30°$. Plotted is the degree of polarization f as a function of the dimensionless time Vt, for two parameter sets: (a) $\omega=0.1V$, $g=5.47$, (b) $\omega=10V$, $g=0.547$. For both sets, $\chi=6V$. Note that in (a), the three figures do not have the same scale for the $f(t)$ coordinate.

tion relation $[\hat{y},\hat{\pi}_y]=i$ and describe a harmonic oscillator of frequency ω. Henceforth, $\hbar$ is set equal to 1. Equation (3) is a particular case of the general Hamiltonian studied in Refs. 1–13.

Our strategy consists in calculating from (3) three observables. The first is the time-resolved $f(t)$ given by (1). The second is the steady-state f_s

$$f_s=\frac{\mathscr{I}_\parallel-\mathscr{I}_\perp}{\mathscr{I}_\parallel+\mathscr{I}_\perp}=\frac{1}{\tau}\int_0^\infty dt\, e^{-t/\tau}f(t), \qquad (4)$$

where $\mathscr{I}_{\parallel,\perp}$ is the total number of photons collected in the detector in the appropriate direction,

$$\mathscr{I}_{\parallel,\perp}=\int_0^\infty dt\, I_{\parallel,\perp}(t), \qquad (5)$$

τ being the excitation lifetime. The third observable is the angle-averaged $\langle f_s\rangle$

$$\langle f_s\rangle=\frac{1}{2\pi}\int_0^{2\pi}f_s(\phi)d\phi. \qquad (6)$$

A comparison of the exact quantum calculation (Refs. 14 and 15) with the consequences of the SCA and the DNLSE then allows us to study in full detail the range of validity of these approximations within the confines of the single-mode sys-

tem described by Eq. (3). We carry out the analysis for zero temperature for simplicity. Work involving finite temperature extensions is under progress and will be the subject of a future publication.

We assume that a frequency-selecting (narrow-band excitation) technique is used in the experiment. This corresponds to low-energy excitation of the composite system. The initial site produced is thus taken to have amplitudes $\cos\phi$ and $\sin\phi$, respectively, of occupation of the two sites, the vibrational component being a displaced oscillator (coherent) state.

In Fig. 2, we plot the degree of polarization $f(t)$ against the dimensionless time Vt computed exactly, and compare it with the result calculated with the SCA and the DNLSE for three representative values of the inclination: $0°$, $15°$, $30°$. The value of the nonlinearity parameter $\chi\equiv 2g^2\omega$ equals $6V$. In (a) $\omega=0.1V$, $g=5.47$, whereas in (b) the parameters are $\omega=10V$, $g=0.547$. In both (a) and (b), as well as throughout this paper, the solid line denotes the result computed exactly, the dotted line is from the result calculated using the SCA and the dashed line is computed using the DNLSE. The agreement between the semiclassical result and the exact result is better in (a) than in (b) and confirms the earlier finding[14] that the SCA improves in accuracy in the infinitely massive oscillator limit $\omega\rightarrow 0$, $g\rightarrow\infty$, $g^2\omega=$const. The oscillations of the semiclassical evolution around the "mean
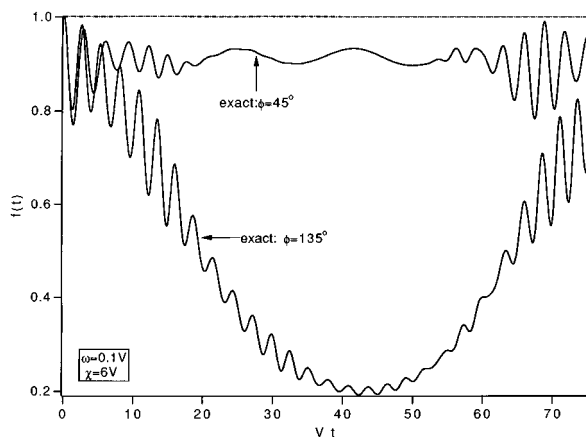
FIG. 3. Comparison of the predictions for time-resolved fluorescence polarization from (i) the exact numerical analysis (solid line), (ii) the semiclassical treatment (dotted line), and (iii) the DNLSE approximation (dashed line) for (a) $\phi=45°$ and (b) $\phi=135°$. The sharp difference between (i) on the one hand and (ii), (iii) on the other stems from the placement of the system in a stationary state in the semiclassical and DNLSE cases but not in the exact quantum mechanical case.

value'' of the exact evolution should be noted. Furthermore, in (b), when the phonon frequency ω becomes large compared to V, the semiclassical result becomes closer to the DNLSE result confirming the standard ``slaving'' argument[22] that the DNLSE obtains from the SCA in the high frequency regime. The effect of initial conditions represented by changing the inclination between the polarization of the incident light and the molecular dipole moment is brought out clearly in Figs. 2(a) and 2(b). Whereas the semiclassical result agrees on the average with the exact result in Fig. 2(a) for 0°, the agreement can change considerably as one changes the angle. For 0°, all the three approaches predict small amplitude oscillations for $f(t)$. For 30° on the other hand, the SCA gives free evolution for $f(t)$ whereas the exact predicts localized behavior. The extent of delocalization shown by the exact result increases as one goes from $\phi=0°$ to $\phi=30°$. This can be understood from the fact that the effective quasiparticle-phonon coupling depends on the population difference between the two sites and it reduces as one increases the polarization angle from $\phi=0°$.[17] It is thus important to note that the effective coupling depends not only on the system parameter g but also on the orientation angle. The fluorescence depolarization experimental technique can change the effective value of the coupling by altering an experimental parameter but without modifying the system parameter.

In Fig. 2(b), for 0°, the agreement between the SCA and the exact result is poor, but gets *better* for 15°. This is in contrast to the tendency in Fig. 2(a). Thus, even the question of validity of the SCA is dependent on the initial angle. Here we see the importance of studying the validity question in the context of specific experimental observables.

Figure 3 shows the degree of polarization $f(t)$ plotted against Vt (as in Fig. 2) using the parameters used in Fig. 2(a) for the inclination ϕ taking the values (a) 45° and (b) 135°. When the angle ϕ takes one of the values 45° and 135°, the semiclassical and the DNLSE systems are initially

placed in a stationary state. For the fully quantum system, however, the vibrational component determines whether the initial state is a stationary state or not. The $f(t)$ computed using SCA and the DNLSE remains at its initial value of 1, whereas the exact $f(t)$ exhibits changes in time.

The study of the steady-state fluorescence f_s is based on the expression in Eq. (4). Figure 4 shows a comparison between f_s computed exactly, from the SCA, and from the DNLSE for the parameter values $\chi=6V$ and $V\tau=0.5$ in (a) and $V\tau=300$ in (b). The case $V\tau=0.5$ represents short-time probing of the dynamics whereas $V\tau=300$ represents the long-time counterpart. The former case is didactic and makes contact with an earlier DNLSE analysis[19] whereas the latter is realistic for many molecular systems: V is of the order of 1 cm^{-1} and τ is of the order of 10^{-8} s. The top figures in (a) and (b) refer to $\omega=0.1V$, the middle figures to $\omega=V$, and the bottom figures to $\omega=10V$. In Fig. 4(a), for $\omega=0.1V$, the agreement between the semiclassical result and the exact result is extremely good whereas the DNLSE result stands apart from the two. The agreement between the SCA and the exact result worsens for larger values of ω, but that between the SCA and the DNLSE improves. The exact result exhibits smooth oscillations. This behavior, which is similar to that of a system with no quasiparticle-phonon coupling, is natural since the coupling constant g is fairly small. It is important to note that the signature of self-trapping, viz., the existence of the two smooth peaks symmetrically placed on either side of $\phi=135°$ is shown by the exact result as well as the two approximations for $\omega=0.1V$. In contrast note that, for $\omega=10V$, since g is so small, the exact evolution no longer exhibits self-trapping and consequently no peaks are observed on either side of $\phi=135°$. As stated earlier,[19] the twin peaks and the ``pinning behavior'' near 135° signify the existence of self-trapped ``stationary states.'' The primary feature of Fig. 4(a) is thus the existence of self-trapped states for small ω shown by the exact evolution and their disappearance for large values of ω. The good agreement between the SCA and the exact result for $\omega=0.1V$ is on account of two factors. First, for times short compared to the tunneling time of the quasiparticle, for small values of ω and large values of g, the semiclassical evolution agrees at least in the average sense with the exact evolution. Secondly, the major discrepancy between the predictions of the semiclassical approximation and the exact evolution really lies in the inability of the semiclassical approximation to predict quasiparticle tunneling. However, owing to the fact that the excitation lifetime τ has been taken to be much shorter than the tunneling time ($\tau=1/2V$ whereas the tunneling time is many orders of magnitude larger), only short-time dynamics are of relevance. The importance of long time dynamics is demonstrated clearly in (b), where $V\tau=300$. There one can see easily that, even for $\omega=0.1V$ (the ``massive oscillator'' regime), the agreement between the SCA and the exact result is rather poor and worsens further with increase in ω. The agreement between the SCA and the DNLSE results for $\omega=10V$ is obtained for $V\tau=300$ also.

It is important to note here that the general semiclassical system has been known to exhibit chaotic behavior[23,24] for certain parameter regimes. We have explored the parameter space and found that Figs. 2 and 3 lie in ``regular islands'' of the system. On the other hand, when one discusses the re-
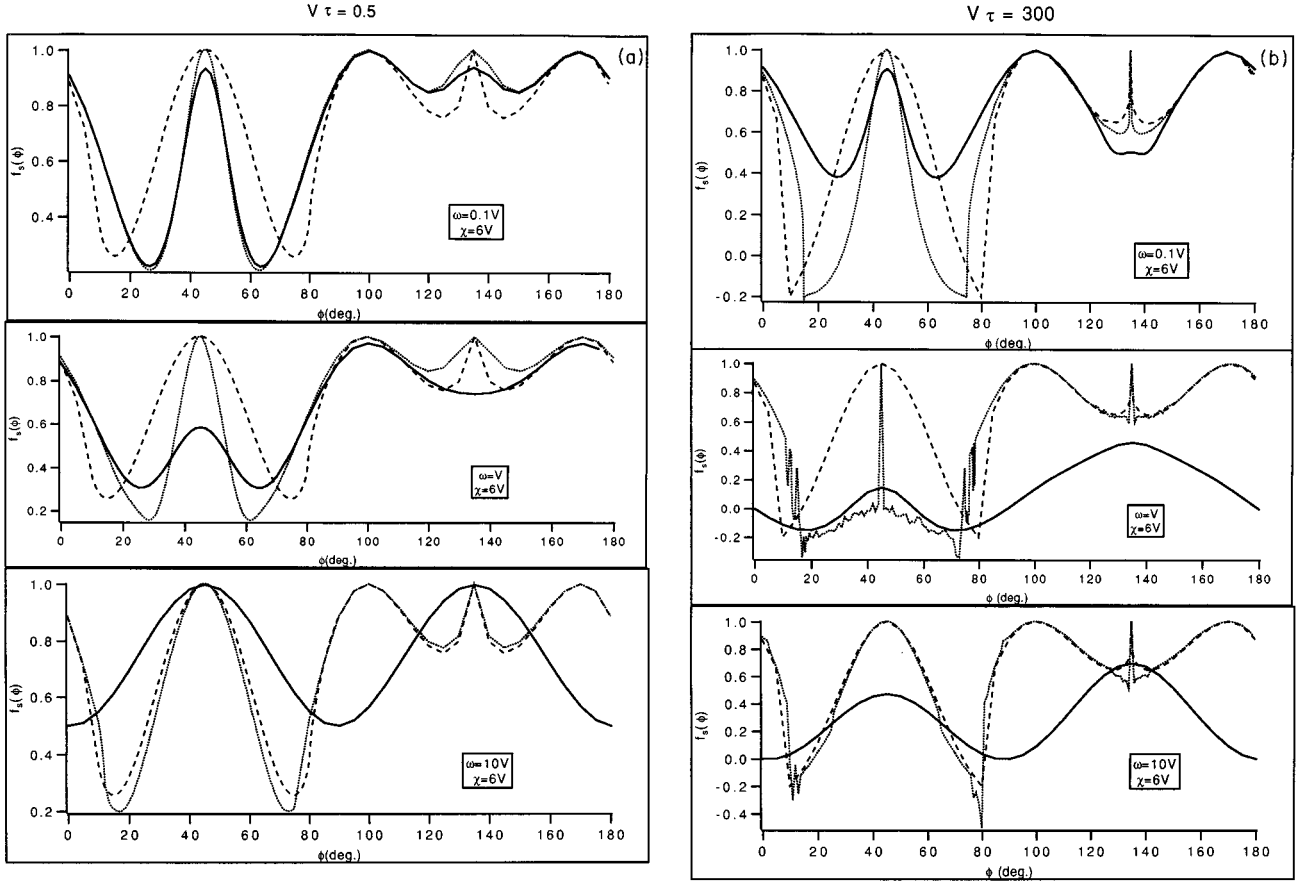
FIG. 4. Comparison of the steady-state fluorescence polarization, f_s computed numerically exactly (solid line), semiclassically (dotted line) and using the DNLSE (dashed line). Shown is the f_s plotted as a function of the orientation angle ϕ, for (a) $V\tau=0.5$ and (b) $V\tau=300$. $\chi=6V$ in both cases. The top figure refers to $\omega=0.1V$, the middle to $\omega=V$, and the bottom to $\omega=10V$.

sults in Fig. 4(b) one traverses various angles and some of those regions do lie in chaotic regimes. This is evident from the irregular behavior of f_s for $\omega=V$ and $\omega=10V$. What emerges from Figs. 4(a) and 4(b) is the following: "irregular" behavior is apparent only from long-time characteristics of the evolution and generally observed for intermediate and high phonon frequencies. There are islands of regular behavior as evidenced by the smooth regions in the behavior of f_s amidst irregular regions. The smooth regions tend to coincide with the behavior of f_s computed from the DNLSE. We emphasize that regular regions correspond to the lower energy part of the spectrum of the system. The spectrum and dynamics are considerably more complicated at higher energies.

One notices from Fig. 4 that the DNLSE and the exact results show similar behavior for f_s when plotted against the polarization angle ϕ especially in the strong-coupling (small ω, finite χ) limit. Many features of the DNLSE system can be understood in terms of a linear nondegenerate dimer[8,9] whose on-site energies are proportional to the initial population difference p_0. For such a *linear* representative dimer system, we find

$$f(t)=\frac{(\Delta p_0-Vr_0)^2}{\Delta^2+V^2}+\frac{(p_0V+\Delta r_0)^2}{\Delta^2+V^2}\cos(2\sqrt{\Delta^2+V^2}t),$$

$$(7)$$

where 2Δ, the energy difference between the two sites, is given by $2c_0p_0V$, c_0 being a dimensionless constant indicating the strength of the disorder in the linear system. The corresponding expression for the steady-state f_s is given by

$$f_s=\frac{(c_0\cos^2 2\phi-\sin^2 2\phi)^2}{1+c_0^2\cos^2 2\phi}$$
$$+\frac{\cos^2 2\phi(1+c_0\sin 2\phi)^2}{(1+c_0^2\cos^2 2\phi)[1+4V^2\tau^2(1+c_0^2\cos^2 2\phi)]}. \quad (8)$$

Figure 5 shows a comparison between the exact result, the DNLSE result and the result obtained from the representative nondegenerate linear dimer model. The parameters for the exact and the DNLSE results are $\omega=0.1V$, $g=3$, $\chi=6V$, whereas those for the linear dimer are $c_0=3$. Figure 4(a) is shown with $V\tau=0.5$ and 4(b) with $V\tau=300$. The DNLSE system and the fully quantum system (particularly for small $V\tau$) are well represented by the linear nondegenerate system. The essential features of the DNLSE system, viz., the stationary state at $\phi=45°$, the splitting of the "metastable stationary state" at $\phi=135°$ to give a self-trapped state, and a sharp difference between the behavior in the region $0°\leq\phi\leq90°$ and the region $90°\leq\phi\leq180°$, are all captured by the representative linear system. We find that the fluores-
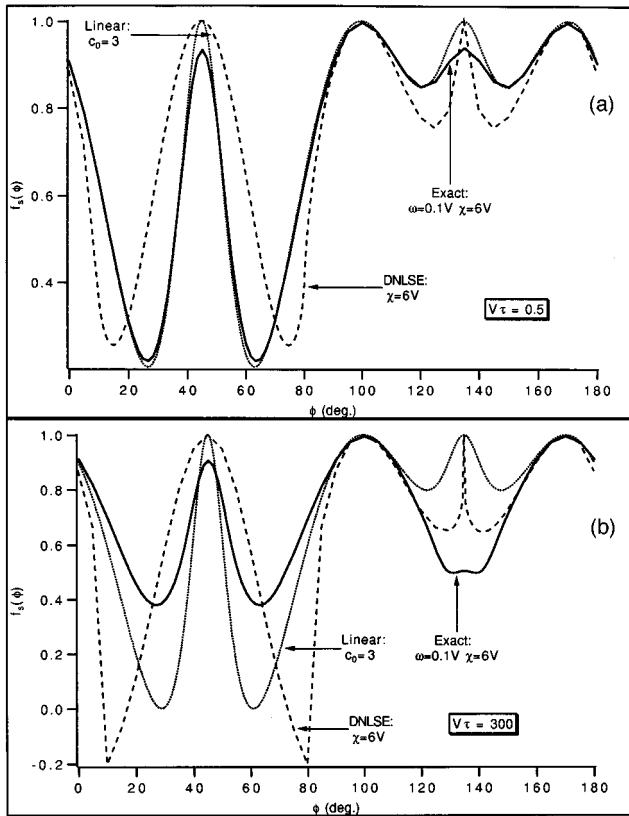
FIG. 5. Comparison of the steady-state fluorescence polarization, f_s computed numerically exactly (solid line), using the DNLSE (dashed line), and the linear nondegenerate model (dotted line) (see text). Shown is the f_s plotted as a function of the orientation angle ϕ, for (a) $V\tau=0.5$ and (b) $V\tau=300$. The exact results and the DNLSE are computed with $\omega=0.1V$, $\chi=6V$ whereas the linear result is calculated with $c_0=3$.

cence depolarization observable in the linear dimer with adjustable nondegeneracy, $c_0\cos2\phi$ displays a sharp transition at $c_0=1$ in complete analogy with the self-trapping transition of the DNLSE system at $\chi=2V$.

The experimental observation of the angle dependence of f_s as shown in Figs. 4 and 5 necessitate the construction of appropriate dimers with definite orientation. Preparation of systems with fixed orientation is difficult in general. Ordinarily encountered stick-dimer systems are solutions in which all orientations are realized. Thus it is often more meaningful to analyze the behavior of steady-state fluorescence averaged over the different orientations or polarization angle defined by Eq. (6). The results for the angle-averaged quantity $\langle f_s\rangle$ are presented graphically in Fig. 6. Since we have shown in Fig. 4 that the semiclassical system exhibits chaos in various parameter regimes, we will display $\langle f_s\rangle$ only for the exact and the DNLSE systems. Corresponding graphs and discussion pertaining to the SCA can be found in Ref. 25. Figure 6(a) shows $\langle f_s\rangle$ plotted against the coupling constant g for three values of ω: $0.1V, V, 10V$ and Fig. 6(b) shows $\langle f_s\rangle$ displayed versus ω in units of V for two values of g: 0.5, 3. In both cases, $V\tau=300$. Two features are of note in (a). The first is the dip shown by the exact result followed by an abrupt crossover for all three values of ω/V. The crossover marks the value of g for which the exact dynamics

shows localization on time scales of the order of $300/V$. The second is the emergence of the static transition shown by the DNLSE at $\chi=2V$ discussed earlier in Refs. 6 and 19: note that the DNLSE stays flat for initial values of g and then rises abruptly. The point at which it rises marks $g^2\omega=V$. It is interesting to note that for large values of ω/V, the exact and approximate solutions approach each other when g is large. Since the SCA and the DNLSE are very close in general for large ω/V, this tendency of the exact and the DNLSE to show similar behavior in this regime for large g reflects the regimes of the validity of the SCA.[14]

The top figure in Fig. 6(b) again displays clearly the DNLSE transition at $\chi\approx2V$. The DNLSE result for $\langle f_s\rangle$ is characterized by a peak at a critical value of χ/V before approaching a value of 0.5 for large χ/V. It is simple to show that this feature is also exhibited by the linear nondegenerate dimer with site energies proportional to the initial population difference. In particular, for large values of $V\tau$, the peak value occurs at $c_0=\sqrt{2(1+\sqrt{2})}$. Since the peak occurs in the DNLSE for equivalently larger values of χ/V, this implies that the peak of the DNLSE $\langle f_s\rangle$ occurs for $\chi/4V>1$ for large $V\tau$.

In summary, the chief outcomes of our investigation of the validity of the SCA and the DNLSE in the specific context of fluorescence depolarization are (i) the SCA improves in validity in the massive oscillator limit $\omega\rightarrow0$, $g\rightarrow\infty$, $g^2\omega=$const., (ii) the SCA tends to the DNLSE in the $\omega\gg V$ limit and to the exact evolution in the $\omega\ll V$ limit (this is clear from the t dependence of the fluorescence signal, the angular dependence of the steady state signal, and the g, ω, and V dependences of the angle-averaged steady-state signal, and is consistent with the massive oscillator limit idea on the one hand and the slaving assumption on the other), (iii) initial conditions have, as expected, a profound effect on the evolution of the system and in particular the degree of polarization f. Varying the angle of inclination works in lieu of varying $g^2\omega$ because it changes the "effective" strength of the coupling.[17] So varying the angle changes the validity of the SCA drastically. Departures from 0° and 90° worsen the agreement. We find that the frequency-resolved absorption of light places the system initially in a stationary state of the dimer *only* for the SCA and the DNLSE but not for the exact evolution. The exact f is time dependent.

For realistic (i.e., large) values of τ, agreement between the exact result and the SCA in the massive oscillator limit becomes worse, the reason being that the steady-state fluorescence picks up long time contributions and at long times (quite apart from quasiparticle tunneling), the evolutions given by the exact approach and the SCA differ significantly. $\langle f_s\rangle$, the angle averaged steady-state signal shows *expected* results for $V\tau=0.5$ but the exact result shows a crossover for $V\tau=300$. The DNLSE result is found to be independent of χ/V until an abrupt transition occurs at a value of χ/V which is approximately 2. Most of the key features of the DNLSE result, including the angle dependence of f_s, and the χ dependence of $\langle f_s\rangle$ can be understood in terms of a linear nondegenerate dimer whose site energies depend on the initial population difference between the two sites.

The initial condition assumed throughout the present study corresponds to a frequency-resolved excitation. Such a situation presupposes a very long duration of the exciting
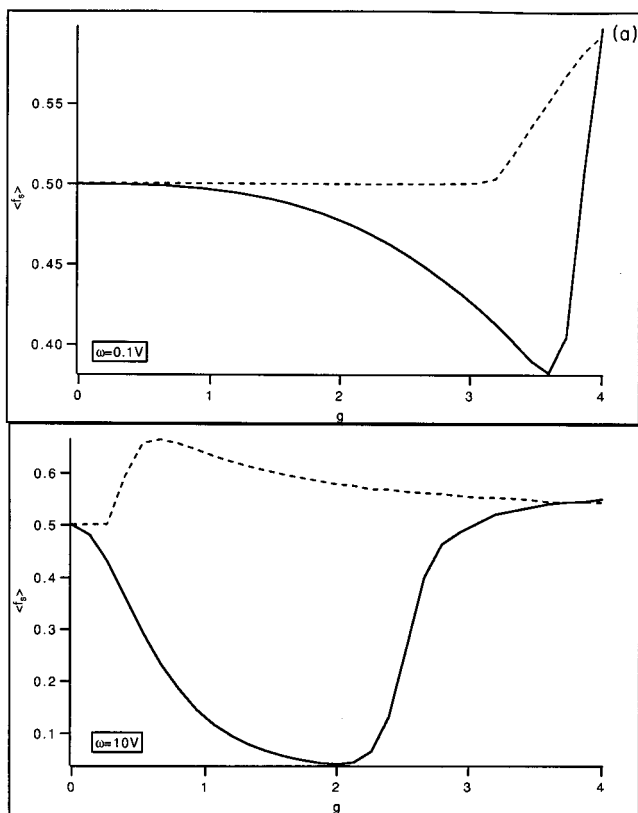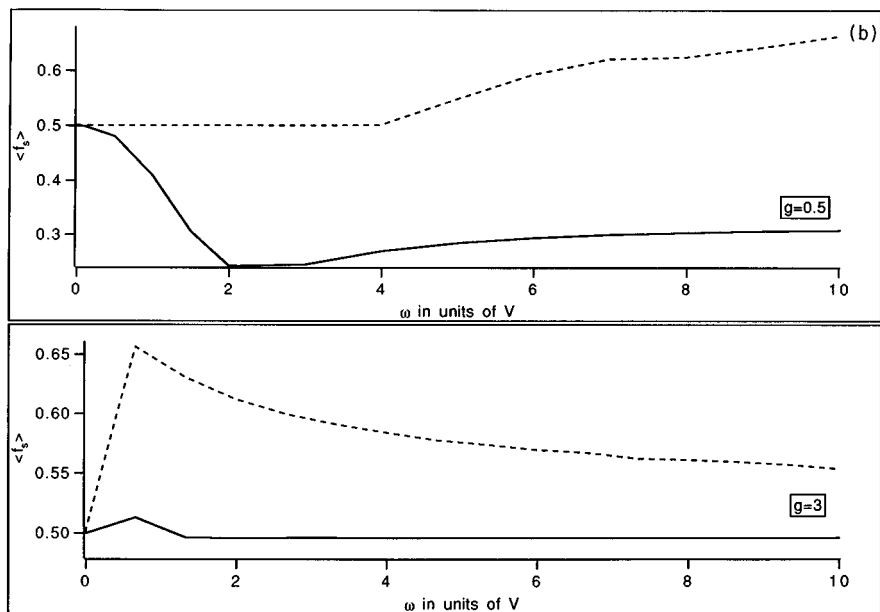
FIG. 6. Comparison of the steady-state fluorescence averaged over orientations calculated numerically exactly (solid line) and using the DNLSE (dashed line). Plotted in (a) is $\langle f_s \rangle$ against g for $\omega = 0.1V, V, 10V$ and in (b) is $\langle f_s \rangle$ against ω in units of V for $g = 0.5, 3$. $V\tau = 300$ in both cases.

pulse. Therefore Figs. 2 and 3 should be considered as primarily serving an illustrative purpose. By contrast, Figs. 4–6, which involve steady-state processes, are realistic. In a forthcoming publication, we will report results for broadband excitation which can be accomplished with pulses of very short duration and which allow fine-scale time resolution. The work reported in the present paper extends our earlier study of the validity of the semiclassical nonlinear equations by including initial condition effects which enter naturally through the variation of the angle of polarization. Work that we have carried out, to be reported in the near future, is an extension in this direction through the study of initial condition in the vibrational space.

*Present address: Department of Physics and Astronomy, McMaster University, Hamilton, Ontario, Canada L8S 4M1.

[1] R. Silbey, Annu. Rev. Phys. Chem. **27**, 203 (1976).

[2] H. Haken and P. Reineker, Z. Phys. **249**, 253 (1972).

[3] V. M. Kenkre, in *Exciton Dynamics in Molecular Crystals and Aggregates*, edited by G. Höhler (Springer, Berlin, 1982).

[4] A. C. Scott, Phys. Rep. **217**, 1 (1992); see also *Davydov's Soliton Revisited: Self-Trapping of Vibrational Energy in Protein*, edited by P. L. Christiansen and A. C. Scott (Plenum, New York, 1990).

[5] J. C. Eilbeck, A. C. Scott, and P. S. Lomdahl, Chem. Phys. Lett. **113**, 29 (1985); Physica D **16**, 318 (1985).

[6] V. M. Kenkre and D. Campbell, Phys. Rev. B **34**, 4959 (1986); V. M. Kenkre, in *Singular Behaviour and Nonlinear Dynamics*, edited by St. Pnevmatikos, T. Bountis, and Sp. Pnevmatikos (World Scientific, Singapore, 1989).

[7] V. M. Kenkre, Physica D **68**, 153 (1993).

[8] V. M. Kenkre and G. P. Tsironis, Phys. Rev. B **35**, 1473 (1987).

[9] G. P. Tsironis and V. M. Kenkre, Phys. Lett. A **127**, 209 (1988).

[10] D. Vitali, P. Allegrini, and P. Grigolini, Chem. Phys. **180**, 297 (1994).

[11] L. Bonci, P. Grigolini, and D. Vitali, Phys. Rev. A **42**, 4452 (1990).

[12] L. Bonci, P. Grigolini, R. Roncaglia, and D. Vitali, Phys. Rev. A **47**, 3538 (1993); L. Bonci, R. Roncaglia, B. J. West, and P. Grigolini, *ibid*. **45**, 8490 (1992); D. Vitali and P. Grigolini, *ibid*. **42**, 7091 (1990); P. Grigolini, Int. J. Mod. Phys. B **6**, 171 (1992).

[13] See also early objections to the semiclassical treatment given by D. Brown, B. West, and K. Lindenberg, Phys. Rev. A **33**, 4110 (1986); D. Brown, K. Lindenberg, and B. West, Phys. Rev. B **35**, 6169 (1987); and by W. C. Kerr and P. S. Lomdahl, *ibid*. **35**, 3629 (1987).

[14] M. I. Salkola, A. R. Bishop, V. M. Kenkre, and S. Raghavan, Phys. Rev. B **52**, 3824 (1995).

[15] V. M. Kenkre, S. Raghavan, A. R. Bishop, and M. I. Salkola, Phys. Rev. B **53**, 5407 (1996).

[16] Note that the SCA in this paper implies the factorization of the expectation values of products of quasiparticle and phonon operators. See also the discussion in Refs. 14 and 15.

[17] V. M. Kenkre, J. Phys. Chem. **98**, 7371 (1994).

[18] T. S. Rahman, R. S. Knox, and V. M. Kenkre, Chem. Phys. **44**, 197 (1979).

[19] V. M. Kenkre and G. P. Tsironis, Chem. Phys. **128**, 219 (1988).

[20] S. Stryer and R. P. Haughland, Proc. Natl. Acad. Sci. U.S.A. **58**, 197 (1967).

[21] K. Wynne and R. M. Hochstrasser, Chem. Phys. **171**, 179 (1993).

[22] See, e.g., V. M. Kenkre and H.-L. Wu, Phys. Rev. B **39**, 6907 (1989); V. M. Kenkre and H.-L. Wu, Phys. Lett. A **135**, 120 (1989).

[23] P. W. Milonni, J. R. Ackerhalt, and H. R. Galbraith, Phys. Rev. Lett. **50**, 966 (1983).

[24] D. Feinberg and J. Ranninger, Physica D **14**, 29 (1984).

[25] S. Raghavan, Ph.D. thesis, University of New Mexico, 1996.